PREDICTION OF CONCENTRATION AND TEMPERATURE DISTRIBUTIONS IN A FLOW REACTOR: HOMOGENEOUS LIQUID-PHASE REACTION

J. A. GOLDING and R. DUSSAULT

Chemical Engineering Department, University of Ottawa, Ottawa, Ontario, Canada

Abstract—A theoretical study has been carried out to evaluate concentration and temperature profiles in a tubular flow reactor. The hydration of acetic anhydride was chosen as the basic reaction and the effects of flow model, reaction kinetics, reaction conditions and variation of system parameters were investigated.

The results showed that radial concentration and temperature profiles were greatly affected by both reaction conditions and flow model. The heat of reaction group, G_4, was found to have the most important effect, such that, in the constant wall-temperature reactor, under laminar flow conditions, large G_4 values increased conversions over those calculated for plug flow conditions. It was also observed under adiabatic reaction conditions that large radial diffusion effects could significantly influence overall conversions. Inlet concentration effects were noted for both the adiabatic and the constant wall-temperature reactors with reaction kinetics significantly affecting reactor performance.

NOMENCLATURE

a, dimensionless radial distance;

A_0, frequency factor in equation (12) $[s^{-1}]$;

A_I, frequency factor for a first-order reaction, equation (3) $[s^{-1}]$;

A_{II}, frequency factor for a second-order reaction, equation (4) $[cm^3 mole^{-1} s^{-1}]$;

C_p, specific heat $[cal/g°K]$;

D_{AM}, effective diffusivity of A in reaction mixture $[cm^2/s]$;

E, activation energy $[cal/g\,mole]$;

G_1, Lewis number as defined by equation (8);

G_2, activation energy group as defined by equation (9);

G_3, frequency factor group as defined by equation (10) or (11);

G_4, heat of reaction group as defined by equation (13) or (14);

ΔH, heat of reaction per mole of reactant A $[cal/g\,mole]$;

k_I, reaction rate constant for a first-order reaction $[s^{-1}]$;

k_{II}, reaction rate constant for a second-order reaction $[cm^3/g\,mole\,s]$;

k_c, thermal conductivity $[cal/s\,cm^2 . °K/cm]$;

r, radial distance $[cm]$;

r_A, reaction rate for component A in equation (1) $[g\,mole/s\,cm^3]$;

r_0, inside tube radius $[cm]$;

R, gas constant $[cal/g\,mole°K]$;

S_c, rate of heat generation by chemical reaction $[cal/s\,cm^3]$;

t, time $[s]$;

T, absolute temperature $[°K]$;

T_0, initial temperature $[°K]$;

u, axial velocity $[cm/s]$;

$\langle u \rangle$, average velocity $[cm/s]$;

x, y, dimensionless concentration as defined in equations (17) and (18);

x_0, inlet mole fraction of component A;

w, dimensionless axial distance as defined in equation (16).

Greek letters

ρ, density $[g/cm^3]$;

ρ_A, concentration of component A $[g\,mole/cm^3]$;

ρ_{A_0}, inlet concentration of component A $[g\,mole/cm^3]$;

ρ_B, concentration of component B $[g\,mole/cm^3]$;

ρ_{B_0}, inlet concentration of component B $[g\,mole/cm^3]$;

θ, dimensionless temperature defined by equation (20);

μ, viscosity $[g/cm\,s]$.

INTRODUCTION

THE PROBLEM of predicting conversions in tubular flow reactors and the effect of mixing and heat transfer has attracted considerable attention in the past [1–6]. These studies have tended to simplify the mathematical analysis as far as possible and the investigations have shown that conversions were affected by velocity profile, axial mixing and temperature rise. Later publications have considered more complex situations studying the effect of velocity profile, reaction conditions and reaction kinetics on concentration and temperature profiles along the reactor and their effect on overall conversions [7–14]. In these investigations the basic differential equations were developed from the general equations of continuity, motion and energy [15]. The equations were then solved using numerical methods.

Rothenberg and Smith [7-8] studied a first-order homogeneous gas-phase reaction taking place in a laminar flow reactor and predicted concentration and temperature profiles. Average "cup-mixing" concentrations and temperatures were also evaluated and the effect of system parameters investigated. The results showed that the temperature rise was extremely dependent on the heat of reaction parameter $-\Delta H \rho_{A0}/\rho C_p T_0$. Similar results were reported by Andersen and Coull [9] who extended their investigation to include adiabatic reaction conditions and compared their conversions to the results that would be obtained for an isothermal plug flow reactor. Investigations studying more practical applications were carried out by Merrill and Hamrin [10], Trombetta and Happel [11] and Lynn and Huff [12]. The authors considered the demethylation of toluene, hydrocarbon pyrolysis and ionic polymerization reactions, respectively. These studies showed that appreciable temperature effects would be expected but no experimental data were presented. Shinohara [14] carried out an experimental and theoretical study of a laminar flow reactor. In developing the theoretical model the temperature dependence of the physical properties was taken into consideration in both the equation of motion and the equation of energy. In the experimental study, cup-mixed exit concentrations and temperatures were measured, but as dilute solutions were employed the influence of the heat of reaction was negligible. Sandru and Smith [16] have studied the photopolymerization of acrylamide in an annular flow reactor; temperature conditions were assumed to be isothermal.

In the present investigation a theoretical study was carried out on the influence of reaction conditions, reaction kinetics, flow conditions and reactant concentration on concentration and temperature profiles in a tubular reactor. The object was to extend the work of previous investigators [8-11] to a more complex second-order liquid-phase reaction. This reaction was chosen as it had the advantage that it would be possible to change reaction kinetics by variation of the concentration of one of the reactants, i.e. pseudo first-order kinetics for dilute solutions and second-order kinetics for more concentrated solutions. A further advantage was that with a liquid-phase reaction it would be easier to obtain experimental data for comparison with theoretical predictions than with a gas-phase reaction. The reference reaction considered in this study was the hydration of acetic anhydride and the parameters used were evaluated for the system acetic anhydride-water-acetic acid. Choice of this system also served to extend the analysis of Cleland and Wilhelm [2] to non-isothermal reaction conditions.

Flow conditions are known to affect concentration and temperature profiles. Three flow models have been studied by previous investigators: (i) plug flow, (ii) laminar or annular flow, and (iii) laminar flow accompanied by radial diffusion. The plug flow model simplifies calculations but can be expected to be inaccurate at low rates particularly if temperature rises are appreciable. The laminar flow model takes into account the residence time distribution at low flow rates and has been used to predict conversion in tubular reactors. Both these models neglect radial flow of material. This can be considered to be the most realistic model with radial flow arising from either molecular or eddy diffusion. However, considerably more computational time is required for this model than for either the plug flow or laminar flow models. Axial diffusion at all times was considered negligible compared to the axial velocity. It should be noticed that for the plug flow model in a constant-wall-temperature reactor radial heat transport will result in radial variations in both temperature and concentration.

THEORETICAL DEVELOPMENT

The differential equations used for prediction of concentration and temperature profiles were developed from continuity and energy equations of Bird et al. [15] assuming constant ρ, μ, k_c and D_{AM}:

$$\frac{D\rho_A}{Dt} = D_{AM}\nabla^2\rho_A + r_A \qquad (1)$$

and

$$\rho\hat{C}_p\frac{DT}{Dt} = k_c\nabla^2 T + S_c. \qquad (2)$$

In writing the energy equation it was assumed heating effects due to expansion, viscous dissipation, free convection and thermodynamic coupling effects are negligible. In addition to develop the final differential equations further simplifying assumptions were also made:

(i) The physical properties of the system can be taken as constant, that is the effects of variation of density, specific heat, thermal conductivity and viscosity on concentration and temperature profiles are negligible compared to the effect of the chemical reaction.

(ii) The variation of reaction rate constant k with temperature can be described using the Arrhenius relationship thus for a first-order reaction $A \rightarrow C$:

$$r_A = -k_1\rho_A = -A_1 e^{-E/RT}.\rho_A \qquad (3)$$

while for a second-order reaction $A + B \rightarrow C$:

$$r_A = -k_{11}\rho_A\rho_B = -A_{11}e^{-E/RT}.\rho_A.\rho_B. \qquad (4)$$

(iii) The heat of reaction can be considered constant over the temperature rises encountered and for an exothermic reaction the rate of evolution of heat due to chemical reaction for the first-order reaction was assumed to be equal to:

$$S_c = \Delta H A_1 e^{-E/RT}.\rho_A \qquad (5)$$

and for the second-order reaction:

$$S_c = \Delta H A_{11}e^{-E/RT}.\rho_A.\rho_B. \qquad (6)$$

(iv) The velocity profiles were constant and fully developed throughout the reactor; then for plug flow $u = \langle u \rangle$ and for laminar flow $u = 2\langle u \rangle [1 - (r/r_0)^2]$. $\qquad (7)$

(v) Axial mass and energy transport due to diffusion and conduction were negligible compared to convective transport.

(vi) The effect of temperature rise on the diffusion coefficient was neglected. In addition stoichiometric diffusion was assumed such that the radial velocity vector could be taken as zero.

NUMERICAL SOLUTION

The derived steady-state differential equations were non-linear and complex, they could not be solved analytically and consequently numerical methods had to be employed. Before deriving the corresponding finite-difference equations the differential equations were written in dimensionless form and the groups and variables selected were the same as those used by previous workers [8-9], namely:

Lewis number, $G_1 = \dfrac{\rho C_p D_{AM}}{k_c}$ (8)

Activation energy group, $G_2 = E/RT_0$ (9)

Frequency factor group,

$$G_3 = r_0^2 \rho C_p A_1/k_c \quad \text{1st-order reaction} \quad (10)$$
$$= r_0^2 \rho C_p A_0/k_c \quad \text{2nd-order reaction} \quad (11)$$

where $A_0 = A_{II}(\rho_{A_0} + \rho_{B_0})$ (12)

Heat of reaction group,

$$G_4 = -\Delta H \rho_{A_0}/\rho C_p T_0 \quad \text{1st-order reaction} \quad (13)$$
$$= -\Delta H(\rho_{A_0} + \rho_{B_0})/\rho C_p T_0$$
$$\text{2nd-order reaction} \quad (14)$$

T_0 = initial or entrance temperature

Radial position, $a = r/r_0$ (15)

Axial position, $w = k_c z/2r_0^2 \langle u \rangle C_p . \rho$ (16)

Dimensionless concentration,

$$x = \frac{\rho_A}{\rho_{A_0}} \quad \text{1st-order reaction} \quad (17)$$

$$y = \frac{\rho_A}{\rho_{A_0} + \rho_{B_0}} \quad \text{2nd-order reaction} \quad (18)$$

$$\Delta y = (\rho_{B_0} - \rho_{A_0})/(\rho_{A_0} + \rho_{B_0}) \quad (19)$$

Dimensionless temperature, $\theta = (T - T_0)/T_0$. (20)

These values were used to develop the required dimensionless continuity and energy equations (21)-(32) shown in Table 1.

It was necessary to modify the differential equations at the centreline of the reactor and at the reactor wall; $a = 0$ and $a = 1$ respectively. At the centreline the conditions imposed at $a = 0$ are shown:

$$\frac{\partial x}{\partial a} \text{ or } \frac{\partial y}{\partial a} = 0, \quad \frac{\partial \theta}{\partial a} = 0. \quad (33)$$

At the reactor wall the boundary conditions depended on both the assumed flow model and the reaction conditions and are shown in Table 2. The equations to be solved were parabolic [17] and the "Crank-Nicholson" method [17-18] was used to develop the required algebraic equations. However at $a = 1$ explicit finite-difference approximations were used [17] to simplify computations. Two sets of algebraic equations were developed which were solved alternately, the calculations being carried out on an IBM 360/65 computer. Firstly, the concentration change was calculated for an axial increment and the corresponding temperature rise evaluated, this temperature rise being required before the next concentration change could be calculated. The procedure was then repeated along the length of the reactor. In determining the concentration profiles for the first-order reaction, computational procedures were straightforward, a standard Gauss-Jordan elimination sub-routine being required for the third flow model. This sub-routine was also employed in determining temperature profiles. In the case of the second-order reaction the numerical equations involved the square of the concentration. This problem

Table 1. Dimensionless continuity and energy equations

Flow model	First-order reaction	Second-order reaction
Plug flow	$\dfrac{dx}{dw} + 2xG_3 e^{-G_2/(\theta+1)} = 0$ (21) $\dfrac{\partial \theta}{\partial w} = 2\left(\dfrac{1}{a}\dfrac{\partial}{\partial a}\cdot\dfrac{a\partial\theta}{\partial a}\right) + 2xG_3.G_4 e^{-G_2/(\theta+1)}$ (22)	$\dfrac{dy}{dw} + 2y(y+\Delta y)G_3.e^{-G_2/(\theta+1)} = 0$ (27) $\dfrac{\partial \theta}{\partial w} = 2\left(\dfrac{1}{a}\dfrac{\partial}{\partial a}\cdot\dfrac{a\partial\theta}{\partial a}\right) + 2y(y+\Delta y)G_3.G_4 e^{-G_2/(\theta+1)}$ (28)
Annular flow	$\dfrac{dx}{dw} + \dfrac{xG_3 e^{-G_2/(\theta+1)}}{(1-a^2)} = 0$ (23) $\dfrac{\partial \theta}{\partial w} = \left(\dfrac{1}{a}\dfrac{\partial}{\partial a}\cdot\dfrac{a\partial\theta}{\partial a}\right) + \dfrac{xG_3.G_4 e^{-G_2/(\theta+1)}}{(1-a^2)}$ (24)	$\dfrac{dy}{dw} + \dfrac{y(y+\Delta y)G_3.e^{-G_2/(\theta+1)}}{(1-a^2)} = 0$ (29) $\dfrac{\partial\theta}{\partial w} = \left(\dfrac{1}{a}\dfrac{\partial}{\partial a}\cdot\dfrac{a\partial\theta}{\partial a}\right) + \dfrac{y(y+\Delta y)G_3.G_4 e^{-G_2/(\theta+1)}}{(1-a^2)}$ (30)
Laminar flow accompanied by radial diffusion	$\dfrac{\partial x}{\partial w} = G_1\left(\dfrac{1}{a}\dfrac{\partial}{\partial a}\cdot\dfrac{a\partial x}{\partial a}\right) - \dfrac{xG_3.G_4 e^{-G_2/(\theta+1)}}{(1-a^2)}$ (25) $\dfrac{\partial \theta}{\partial w} = \dfrac{1}{(1-a^2)}\left(\dfrac{1}{a}\dfrac{\partial}{\partial a}\cdot\dfrac{a\partial\theta}{\partial a}\right) + \dfrac{xG_3.G_4 e^{-G_2/(\theta+1)}}{(1-a^2)}$ (26)	$\dfrac{\partial y}{\partial w} = G_1\left(\dfrac{1}{a}\dfrac{\partial}{\partial a}\cdot\dfrac{a\partial y}{\partial a}\right) - \dfrac{y(y+\Delta y)G_3.G_4 e^{-G_2/(\theta+1)}}{(1-a^2)}$ (31) $\dfrac{\partial\theta}{\partial w} = \dfrac{1}{(1-a^2)}\left(\dfrac{1}{a}\dfrac{\partial}{\partial a}\cdot\dfrac{a\partial\theta}{\partial a}\right) + \dfrac{y(y+\Delta y)G_3.G_4 e^{-G_2/(\theta+1)}}{(1-a^2)}$ (32)

Table 2. Wall boundary conditions

Flow model	Adiabatic reaction	Constant-wall-temperature reactor
Plug flow	$\dfrac{\partial \theta}{\partial a} = 0$ $a = 1$	$\theta = 0$ $a = 1$
Laminar flow	$x = 0, \ y = 0, \ \dfrac{\partial \theta}{\partial a} = 0$ $a = 1$	$x = 0, \ y = 0, \ \theta = 0$ $a = 1$
Laminar flow accompanied by radial diffusion	$\dfrac{\partial x}{\partial a}, \dfrac{\partial y}{\partial a} = 0, \ \dfrac{\partial \theta}{\partial a} = 0$ $a = 1$	$\dfrac{\partial x}{\partial a}, \dfrac{\partial y}{\partial a} = 0, \ \theta = 0$ $a = 1$

was overcome for plug flow and laminar flow by only taking the positive root and putting $y = 0$ when both roots became negative. For the case of laminar flow accompanied by diffusion the above technique could not be used and an iterative method had to be employed. Two to three iterations were required for each axial increment. Bulk or "cup-mixing" concentrations and temperatures were computed from the radial concentration and temperature profiles respectively using Simpson's rule to evaluate the integral. Other numerical methods using Romberg's integration and the Gauss quadrature were investigated but showed only marginal improvement or were inferior to Simpson's rule [19]. Numerical calculations were then carried out to determine the effects of varying the parametric groups, reaction conditions, reaction kinetics and inlet reactant concentration on conversions and temperature rises along the reactor.

RESULTS

Adiabatic-reaction conditions

Before carrying out detailed numerical computations a check was made with the results reported in the literature [8, 9] for a first-order reaction taking place in a constant-wall-temperature reactor. Calculations predicting the variation of both cup-mixing temperatures, $\langle \theta \rangle$ and cup-mixing concentrations, $\langle x \rangle$ with the axial distance, w, were compared. Agreement was good and in addition the instabilities reported by Rothenberg [8] for G_4 values greater than 0·37 were eliminated. In addition a comparison was also made with the results reported by Cleland and Wilhelm for the hydration of dilute solutions of acetic anhydride under isothermal conditions, agreement was very good.

In comparing results it was found to be more convenient to plot $\langle x \rangle$ rather than $\langle y \rangle$ for the second order reaction and the variation of $\langle \theta \rangle$ and $\langle x \rangle$ with w for the different flow models for a reaction carried out under adiabatic conditions are shown in Fig. 1. The computations indicated that for all the flow models the reaction was characterized by a rapid decrease in reactant concentration with increasing w. The reaction rate increased rapidly due to the accompanying temperature rise until the completion of the reaction. For

all flow models the final adiabatic dimensionless temperature was 0·19 as required from an overall energy balance. A comparison of the flow models showed that conversion rates were considerably greater under plug flow conditions than for laminar flow conditions (Fig. 1). Radial diffusion was also observed to influence overall conversion rates (Fig. 1) and was further studied by varying G_1. It was found that although molecular
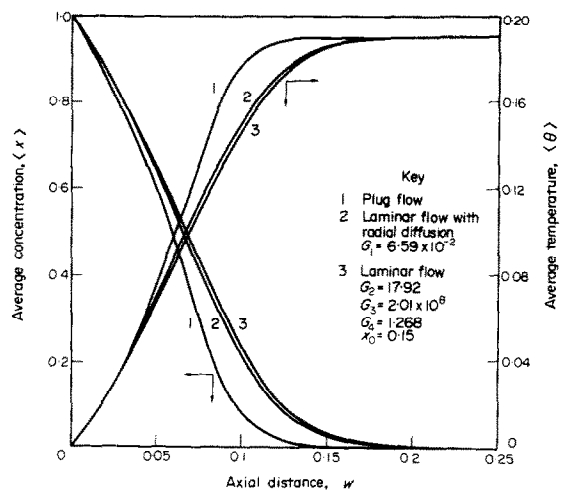

Key
1 Plug flow
2 Laminar flow with radial diffusion $G_1 = 6·59 \times 10^{-2}$
3 Laminar flow $G_2 = 17·92$ $G_3 = 2·01 \times 10^8$ $G_4 = 1·268$ $x_0 = 0·15$

FIG. 1. Effect of flow model on conversion, $\langle x \rangle$, and temperature rise, $\langle \theta \rangle$. Second order reaction, adiabatic reaction conditions.

diffusion $(G_1 = 0·000659)$ would not influence conversions, any significant movement of reactant in the radial direction would appreciably increase conversion rates (Fig. 2).

In determining the effects of G_2 and G_3 the product $G_3 e^{-G_2}$ was kept constant at 3·316. The results were similar to those found by previous investigators for a constant-wall-temperature reactor: the reaction rate being more dependent on the energy of activation group, G_2, than on the frequency group, G_3. The heat of reaction group, G_4, greatly affected reaction rates (Fig. 3): reaction rates increasing rapidly with increase in G_4. The influence of flow model was again apparent;
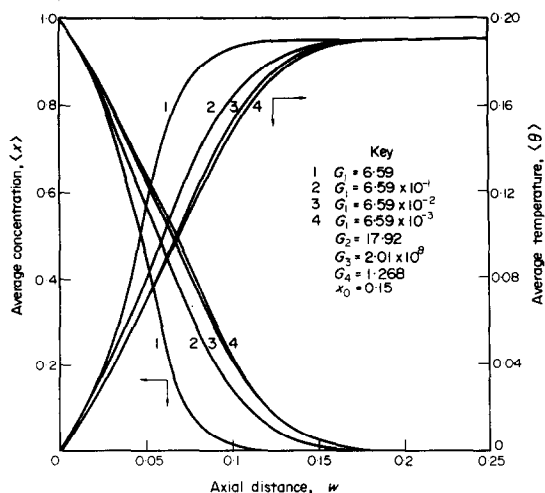
FIG. 2. Effect of radial material transport on conversion, $\langle x \rangle$, and temperature rise, $\langle \theta \rangle$. Second order reaction, adiabatic reaction conditions.
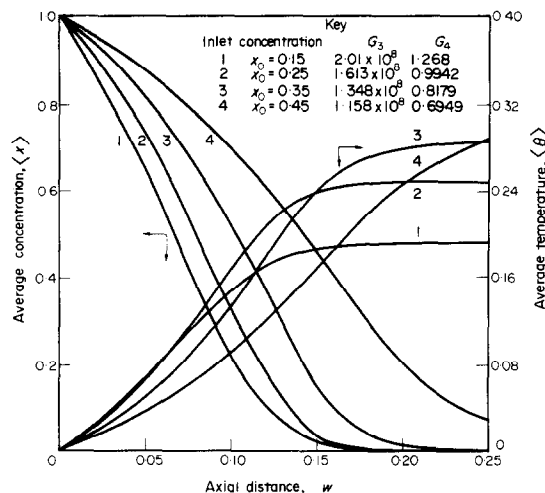

FIG. 4. Effect of inlet concentration on conversion, $\langle x \rangle$, and temperature rise, $\langle \theta \rangle$. Second order reaction, adiabatic reaction conditions. Laminar flow model, $G = 17.92$.
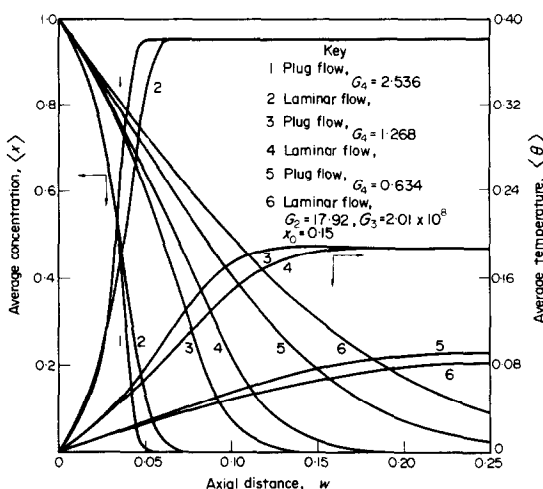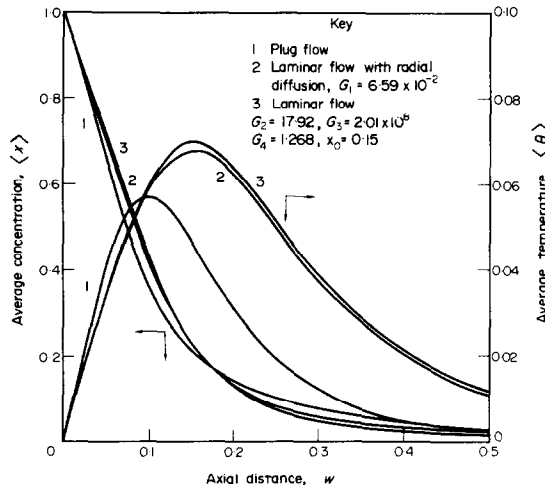

FIG. 3. Effect of the heat of reaction group, G_4, and flow model on conversion, $\langle x \rangle$, and temperature rise, $\langle \theta \rangle$. Second order reaction, adiabatic reaction conditions.

FIG. 5. Effect of flow model on conversion, $\langle x \rangle$, and temperature rise, $\langle \theta \rangle$, in a constant wall-temperature reactor. Second order reaction.

the difference in conversion for the laminar flow and plug flow model being more marked as G_4 values were lowered (Fig. 3). For an endothermic reaction (G_4 negative), reaction rates decreased as the reaction proceeded and for very large values of G_4 computations indicated that the reaction should come to a virtual halt.

Varying the inlet reactant concentration ρ_{A_0} affected the overall conversion and the final temperature. Reaction rates initially increased but then decreased as ρ_{A_0} was increased as a result of the accompanying decrease in ρ_{B_0}. This decrease in ρ_{B_0} was not always compensated for by the increase in reaction rate due to the temperature rise (Fig. 4). Consequently, for a given length reactor the percentage conversion could decrease as the concentration ρ_{A_0} was raised. This effect of concentration on percent conversions was also pronounced for a constant wall-temperature reactor as discussed later.

Constant-wall-temperature reactor

In a constant wall-temperature reactor the cup-mixed temperatures were found to exhibit characteristic maxima as the reaction proceeded (Fig. 5). The effect of flow model is also shown in Fig. 5, the predicted maximum temperature being appreciably smaller in plug flow than in laminar flow. It is interesting to note that due to the larger maximum cup-mixed temperatures reached in laminar flow overall conversion rates are slightly higher in laminar flow than in plug flow. When the effect of radial transport was studied by varying G_1, the maximum temperature decreased as G_1 increased and the results tended towards those predicted for the plug-flow reactor. When G_4 was varied the calculations showed that as G_4 values rose there would be an accumulation of heat in the initial section of the reactor which would result in very high maximum temperatures and consequent acceleration of the reaction. The effect of G_4 on conversions is
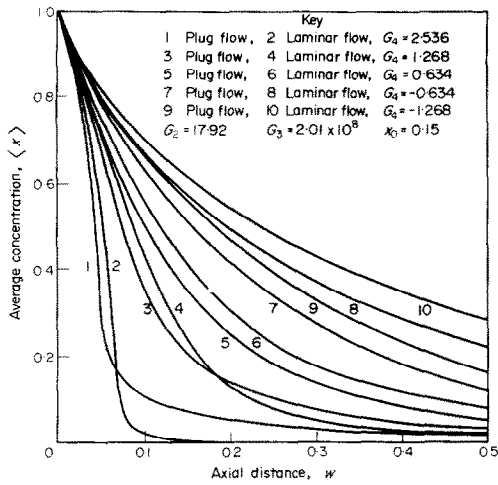
FIG. 6. Effect of the heat of reaction group, G_4, and flow model on conversion, $\langle x \rangle$, in a constant wall-temperature reactor. Second order reaction.
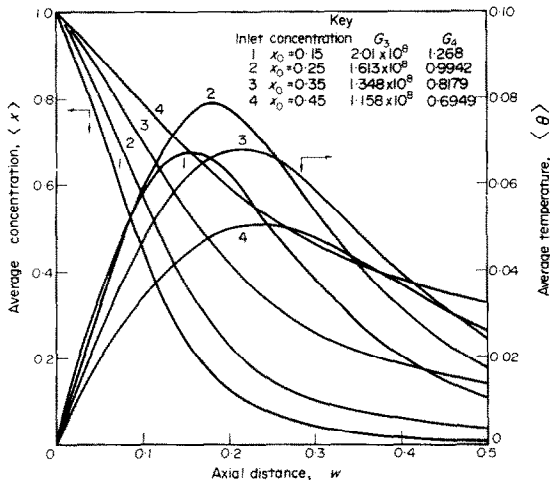

FIG. 7. Effect of inlet concentration on conversion, $\langle x \rangle$, and the temperature rise, $\langle \theta \rangle$, in a constant wall-temperature reactor. Second order reaction. Laminar flow with radial diffusion, $G_1 = 0.0659$.
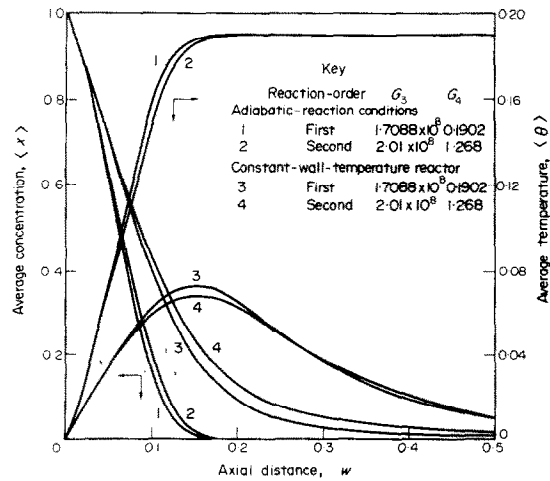

FIG. 8. Effect of reaction order on conversion, $\langle x \rangle$, and temperature rise, $\langle \theta \rangle$, in a tubular reactor. Laminar flow with radial transport, $G_1 = 0.0659$. $G_2 = 17.92$. $x_0 = 0.15$ mole fraction component A.

shown in Fig. 6 and a varied effect of flow pattern on conversion was also observed. Thus for high values of G_4 overall conversion could be greater under laminar flow condition than for plug flow conditions, but as heat effects became less important the plug flow reactor was much more efficient. This latter effect has been predicted for an isothermal flow reactor [9] and was found in this study to be particularly pronounced for endothermic reactions (Fig. 6). It should be noted that for the constant wall-temperature reactor, that depending on the reaction, high temperature rises taking place in laminar flow can also lead to undesirable product degradation rather than an increase in conversion. The effect of inlet concentration was similar to the effects calculated for adiabatic reaction conditions thus the maximum temperature initially rose as ρ_{A_0} was increased then decreased due to the decrease in ρ_{B_0} (Fig. 7). This resulted in a decrease in the fractional conversion along the reactor as ρ_{A_0} was raised (Fig. 7).

When the calculations were carried out assuming first-order kinetics, reaction rates were found to be faster under all reaction conditions. This resulted in an increase in fraction conversion with w and led to larger temperature rises in the constant wall-temperature reactor (Fig. 8). The calculations also showed that for a first-order reaction the effect of flow model on $\langle x \rangle$ and $\langle \theta \rangle$ lessened when compared to the effects observed for a second-order reaction. The effect of reaction kinetics on overall conversions was emphasized when the inlet concentration ρ_{A_0} was increased.

Radial profiles

The radial profiles depended on both flow model and reaction conditions. Under adiabatic reaction conditions and for plug flow the concentrations and temperatures were constant in the radial direction but under laminar flow conditions the profiles varied widely with the radial distance, a. Thus the reactant concentration fell rapidly at the wall with a maximum reactant concentration being established at the centre of the reactor. Then as the reaction proceeded and the reactant depleted, the profile gradually flattened (Fig. 9). The corresponding temperature profiles for the laminar flow reactor are shown in Fig. 10. A maximum temperature was first found at the reactor wall and then moved towards the centre of the reactor as the reaction proceeded. Point temperatures in excess of the theoretical adiabatic temperature were found due to radial transport of material. When the effect of G_1 was studied radial transport of material tended to flatten the profiles.

In contrast, for the constant wall-temperature reactor concentration profiles were of approximately the same shape under laminar flow conditions as those found for the adiabatic reactor. However, for the plug-flow reactor the model predicted a depletion of reactant concentration at the centre of the reactor opposite to that predicted for laminar flow (Fig. 11). In the case of the temperature profiles the plug flow model always predicted a maximum at the centre of the reactor. But under laminar flow conditions calculations showed that
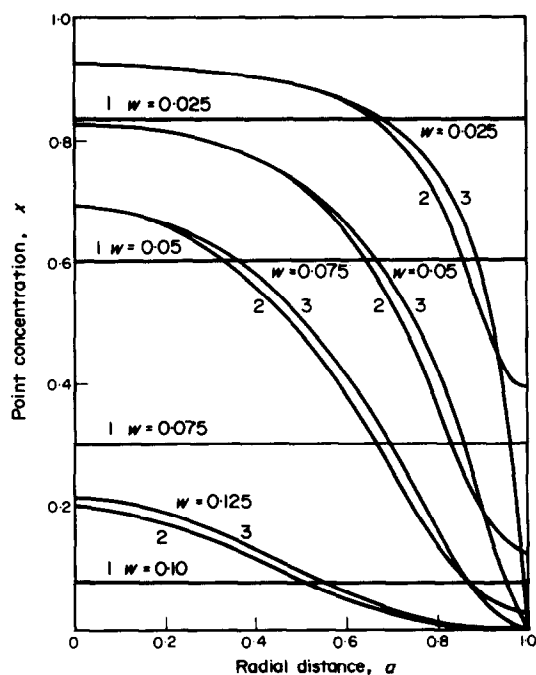
FIG. 9. Radial concentration profiles along the reactor. Second order reaction, adiabatic reaction conditions: (1) Plug flow. (2) Laminar flow with radial diffusion, $G_1 = 0.0659$. (3) Laminar flow, $G_2 = 17.92$, $G_3 = 2.01 \times 10^8$, $G_4 = 1.268$.

FIG. 11. Radial concentration profiles along a constant wall-temperature reactor. First order reaction: (1) Plug flow. (2) Laminar flow with radial diffusion, $G_1 = 0.0659$. (3) Laminar flow, $G_2 = 17.92$, $G_3 = 1.7088 \times 10^8$, $G_4 = 0.1902$.

there was very little effect of flow model on maximum point temperatures reached in a flow reactor even though maximun "cup-mixed" temperatures differed appreciably under laminar and plug flow conditions.

SUMMARY

Calculations carried out to determine the effects of system parameters, flow model, reaction kinetics and reaction conditions have shown that flow model not only influences concentration and temperature profiles but overall conversions as well. Higher overall conversions are usually obtained in plug flow, but for a constant wall-temperature reactor conversion rates can be enhanced under laminar flow conditions when large temperature effects are present. Although normally molecular diffusion would not be expected to influence profiles, conversions can be significantly affected if radial movement of material takes place. For the constant wall-temperature reactor point temperatures can be significantly larger than cup-mixed temperatures particularly under plug flow conditions. Reactant concentration and reaction kinetics were observed to affect overall conversion rates and temperature rises. The influence of these variables was generally greater for the constant wall-temperature reactor than for a reaction carried out under adiabatic reaction conditions. Concentration and temperature profiles were found to be influenced by both reaction conditions and flow model. Under laminar flow conditions maximum temperatures initially arose at an intermediate radial position before the maximum was established at the reactor centreline. This effect was very pronounced for a reaction carried out under adiabatic reaction conditions.
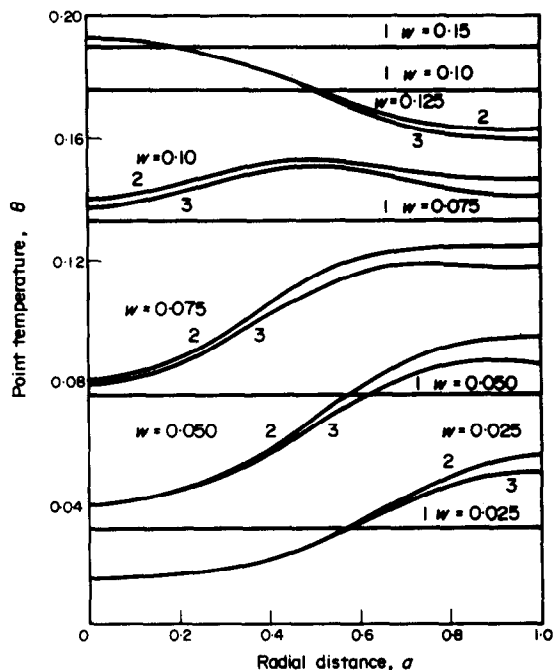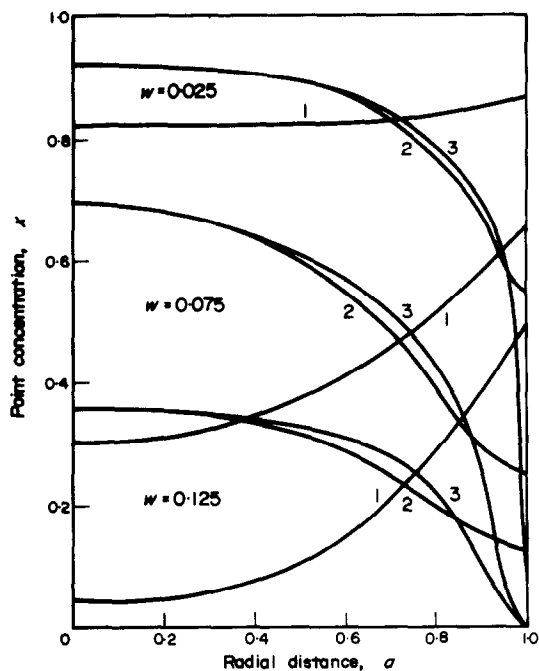

FIG. 10. Radial temperature profiles along the reactor. Second order reaction, adiabatic reaction conditions: (1) Plug flow. (2) Laminar flow with radial diffusion, $G_1 = 0.0659$. (3) Laminar flow, $G_2 = 17.92$, $G_3 = 2.01 \times 10^8$, $G_4 = 1.268$.

initially the maximum temperature should appear at an intermediate radial position before being established at the centre of the reactor. The calculations also showed that for all flow models maximum point temperatures were much higher than the maximum cup-mixed temperatures. The calculations indicated however that

REFERENCES

1. P. L. Chambré, On chemical reactions in internal flow systems, *Appl. Scient. Res.* **A9**, 157 (1960).
2. F. A. Cleland and R. H. Wilhelm, Diffusion and reaction in viscous-flow tubular reactor, *A.I.Ch.E. Jl* **2**, 489 (1956).
3. K. G. Denbigh, *Chemical Reactor Theory*, Vol. 1, Chapter 2. Cambridge University Press, London (1965).
4. J. P. Irving and J. M. Smith, Heat transfer in a chemically reacting system (nitrogen tetroxide–dioxide), *A.I.Ch.E. Jl* **7**, 91 (1961).
5. J. P. Vignes and P. J. Trambouze, Diffusion and chemical reaction in a laminar-flow tubular reactor, *Chem. Engng Sci.* **17**, 73 (1962).
6. J. F. Wehner and R. H. Wilhelm, Boundary conditions of flow reactor, *Chem. Engng Sci.* **6**, 89 (1956).
7. R. I. Rothenberg and J. M. Smith, Dissociation and heat transfer in laminar flow, *Can. J. Chem. Engng* **44**, 67 (1966).
8. R. I. Rothenberg and J. M. Smith, Heat transfer and reaction in laminar tube flow, *A.I.Ch.E. Jl* **12**, 213 (1966).
9. T. S. Andersen and J. Coull, Evaluation of models for tubular, laminar flow reactors, *A.I.Ch.E. Jl* **16**, 542 (1970).
10. L. S. Merrill, Jr. and C. E. Hamrin, Jr., Conversion and temperature profiles for complex reactions in laminar and plug flow, *A.I.Ch.E. Jl* **16**, 194 (1970).
11. M. L. Trombetta and J. Happel, Analysis and design of gas flow reactors with applications to hydrocarbon pyrolysis, *A.I.Ch.E. Jl* **11**, 1041 (1965).
12. S. Lynn and J. E. Huff, Polymerization in a tubular reactor, *A.I.Ch.E. Jl* **17**, 475 (1971).
13. R. K. Nilsen and C. E. Hamrin, Jr., Tubular reactors: effect of flow profile on conversion for a nonelementary reaction, *A.I.Ch.E. Jl* **17**, 1497 (1971).
14. T. Shinohara, An experimental and theoretical study of a laminar-flow tubular reactor, Ph.D. Thesis, University of Utah (1972).
15. R. B. Bird, W. E. Stewart and E. N. Lightfoot, *Transport Phenomena*. John Wiley, New York (1960).
16. D. Sandru and J. M. Smith, Photopolymerization of acrylamide in an annular flow reactor, *A.I.Ch.E. Jl* **19**, 558 (1973).
17. L. Lapidus, *Digital Computation for Chemical Engineers*, Chapter 4. McGraw-Hill, New York (1962).
18. V. G. Jensen and G. V. Jeffreys, *Mathematical Methods in Chemical Engineering*, p. 420. Academic Press, New York (1963).
19. R. J. Lemay, Prediction of concentration and temperature profiles in a conical flow reactor. B.A.Sc. Thesis, University of Ottawa, Ottawa (1974).

PREVISION DES DISTRIBUTIONS DE CONCENTRATION ET DE TEMPERATURE DANS UN REACTEUR CONTINU: REACTION HOMOGENE EN PHASE LIQUIDE

Résumé—On étudie par voie théorique les profils de concentration et de température dans un réacteur continu tubulaire. On a choisi comme réaction l'hydratation de l'anhydride acétique et on étudie les effets du modèle d'écoulement, de la cinétique de réaction, des conditions de réaction et de la variation des paramètres du système.

Les résultats montrent que les profils radiaux de concentration et de température sont fortement sensibles à la fois aux conditions de réaction et au modèle de l'écoulement. Le groupe de chaleur de réaction G_4 a l'effet le plus important, si bien que dans un réacteur à température pariétale constante et pour des conditions d'écoulement laminaire, de fortes valeurs de G_4 accroissent les conversions au dessus de celles calculées dans des conditions d'écoulement piston. On constate aussi, pour des condiions de réaction adiabatique, que des effets importants de diffusion radiale peuvent influencer de façon significative les conversions globales. Pour les réacteurs adiabatiques ou à température pariétale constante, on note des effets sensibles de la concentration à l'entrée sur les performances du réacteur à travers la cinétique de réaction.

BERECHNUNG DER KONZENTRATIONS-UND TEMPERATURVERTEILUNGEN IN EINEM FLIESSREAKTOR: HOMOGENE FLÜSSIG-PHASEN-REAKTION

Zusammenfassung—Zur Berechnung der Konzentrations- und Temperaturprofile in röhrenförmigen Fließreaktoren wurde eine theoretische Untersuchung durchgeführt. Die Hydration von Essigsäure-Anhydrid wurde als Grundreaktion gewählt und die Einflüsse des Strömungsmodells, der Reaktionskinetik, der Reaktionsbedingungen und der Änderungen der Systemparameter wurden untersucht. Die Ergebnisse zeigten, daß die Radialkonzentration und die Temperaturprofile stark beeinflußt wurden, sowohl durch die Reaktionsbedingungen wie auch durch das Strömungsmodell. Die Reaktionswärme G_4 hatte den wichtigsten Einfluß, so daß in einem Reaktor mit konstanter Wandtemperatur bei laminarer Strömung große Werte von G_4 die Konversion auf Werte anhob, die über jenen für Pfropfenströmung lagen. Unter adiabaten Reaktionsbedingungen zeigte sich auch, daß große Radialdiffusionseinflüsse, die Gesamtkonversionsraten deutlich verändern können. Einlauf-Konzentrationseffekte zeigten sich sowohl für den adiabaten, als auch für den Reaktor mit konstanter Wandtemperatur, wobei die Reaktionskinetik das Reaktorverhalten deutlich beeinflußte.

РАСЧЕТ РАСПРЕДЕЛЕНИЯ КОНЦЕНТРАЦИИ И ТЕМПЕРАТУРЫ В ПРОТОЧНОМ РЕАКТОРЕ: ГОМОГЕННАЯ РЕАКЦИЯ В ЖИДКОЙ ФАЗЕ

Аннотация — Проведено теоретическое исследование по расчету профилей температуры и концентрации в проточном трубчатом реакторе. В качестве модельной реакции была выбрана гидратация уксусного ангидрида. На её примере исследовалось влияние модели течения, кинетики реакции, условий реакции и изменения параметров системы.

Полученные результаты показали, что радиальные профили концентрации и температуры зависят как от условий протекания реакции, так и от модели течения. Было обнаружено, что наибольшее влияние оказывает тепло реакционной группы G_4. В частности, в условиях ламинарного течения в реакторе с постоянной температурой стенок при больших значениях G_4 конверсия была выше вычисленной для условий снарядного течения. Было обнаружено, что при адиабатических условиях реакции эффекты сильной радиальной диффузии могут значительно влиять на общую конверсию. Влияние начальной концентрации было отмечено как для адиабатических реакторов, так и для реакторов с постоянной температурой стенок, причем кинетика реакции значительно влияла на функционирование реактора.